

Vacuum Window Design for High Power Lasers

T. Shaftan,
NSLS, Brookhaven National Laboratory, Upton, NY

August, 2005

National Synchrotron Light Source
Brookhaven National Laboratory
P.O. Box 5000
Upton, NY 11973

DISCLAIMER

This report was prepared as an account of work sponsored by an agency of the United States Government. Neither the United States Government nor any agency thereof, nor any of their employees, nor any of their contractors, subcontractors or their employees, makes any warranty, express or implied, or assumes any legal liability or responsibility for the accuracy, completeness, or any third party's use or the results of such use of any information, apparatus, product, or process disclosed, or represents that its use would not infringe privately owned rights. Reference herein to any specific commercial product, process, or service by trade name, trademark, manufacturer, or otherwise, does not necessarily constitute or imply its endorsement, recommendation, or favoring by the United States Government or any agency thereof or its contractors or subcontractors. The views and opinions of authors expressed herein do not necessarily state to reflect those of the United States Government or any agency thereof.

Vacuum window design for high-power lasers

Abstract

One of the problems in the high-power lasers design is in outcoupling of a powerful laser beam out of a vacuum volume into atmosphere. Usually the laser device is located inside a vacuum tank. The laser radiation is transported to the outside world through the transparent vacuum window. While considered transparent, some of the light passing through the glass is absorbed and converted to heat. For most applications, these properties are academic curiosities; however, in multi-kilowatt lasers, the heat becomes significant and can lead to a failure. The absorbed power can result in thermal stress, reduction of light transmission and, consequently, window damage. Modern optical technology has developed different types of glass (Silica, BK7, diamond, etc.) that have high thermal conductivity and damage threshold. However, for kilo- and megawatt lasers the issue still remains open.

In this paper we present a solution that may relieve the heat load on the output window. We discuss advantages and issues of this particular window design.

Introduction



Fig. 1: An example of the stress fracture of an optical element.



Fig. 2: An example of a fracture due to contamination of an optical element surface.

Conventional laser technology provides with a variety of optics for high-power laser applications. Modern high-power CO₂ lasers reach 50 kW level of power¹. At this power level the laser optics must be transparent in a large range (for tunable lasers) and have high damage threshold. Two examples² of optical element damage are shown in Fig. 1 and 2.

¹ http://www.linde-gas.com/International/Web/LG/COM/like1gcomn.nsf/DocByAlias/ind_mv_laser1

² Figures from: <http://www.lightpath.com/PDF Files/White Papers/LPT white paper.pdf>

In this note we assume (as an example) 100 kW cw IR laser beam passing through a window with 20 cm diameter. Distribution of the power per unit area is given in the next figure (Fig. 3).

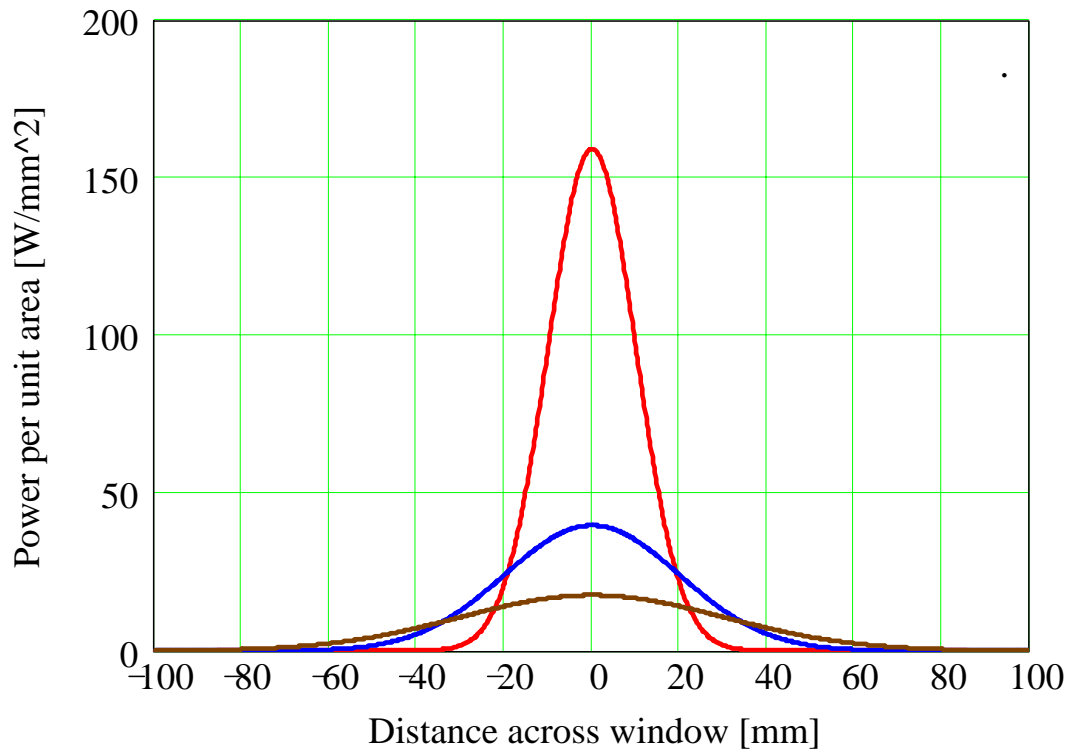


Fig. 3: Power [W/mm²] for three beam sizes of 1, 2 and 3 cm RMS.

These power levels may be dangerous for the laser optics. Vacuum window is one of the main concerns, since its damage may cause vacuum leak and, in turn, failure of a laser performance.

In this note we discuss an approach for reducing heat load on unit surface for a vacuum window of a high-power laser. First, we review a vacuum foil design in industrial accelerators. In the following we discuss similar approach in high-power laser case. Next we suggest certain design and estimate its thermal and optical properties. In conclusion we review a future work.

Industrial accelerator technology

Industrial accelerators provide with few MW power electron beams. Special extraction device (BINP, Russia) is being used in order to separate vacuum volume and atmosphere (Fig. 4).

Extraction device with a foil window³

“The schematic diagram of the device designed for the beam extraction into air through the foil is given in Fig.8. An electron beam is scanned over the foil in two mutually perpendicular directions with the use of two electromagnets. The scanning frequencies have the ratio 251/15. Due to this, there is no overlapping of beam trajectories and the foil is filled completely. The beam of low frequency is scanned along the foil and the beam of high frequency is scanned across the foil. The scanning frequency along the foil is about of 50 Hz, if there are no special technological requirements. The maximum deflection angle of a beam is 30°.

The foil is cooled with an air jet. To this end, the high-pressure fan is used with the preliminary rate of the jet of 180-200 km/h. At this rate, an average density of current on the foil does not exceed 100 mA/cm², i. e. maximum extracting current value is 70 mA/m. This is approximately twice as smaller as the maximum admissible value for the current density on the foil for this jet rate. This double reserve of current density throughout the foil makes its lifetime practically limitless. Fig.4 shows the distribution of the linear density of a current at a distance of 50 mm from the frame of extraction window. The linear density of current is a part of the beam measured by the long probe installed across the extraction window. The value of the absorbed dose in the irradiated material is proportional namely to this parameter. Usually, we guarantee an inhomogeneity of the current linear density of no worse than ±10 % at a distance no more than 50 mm with the 90 % use of the beam current. The current losses on the distribution tails are caused by the electron scattering on the extraction window foil and in air.

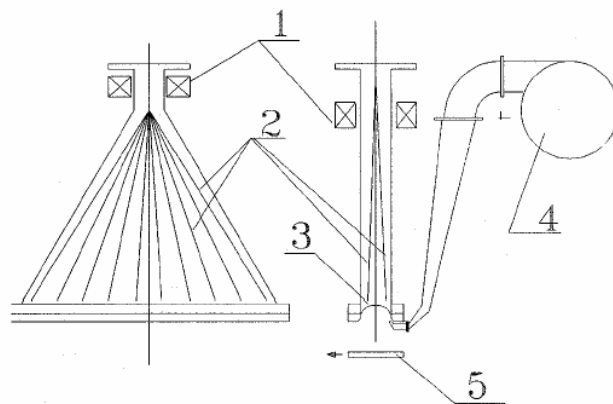


Fig: 4: Vacuum foil design in the industrial accelerator. 1 – scanning electromagnets, 2 - beam trajectories; 3 - foil of extraction window; 4 - foil cooling fan; 5 - movable target”

³ Quoted from: <http://www.inp.nsk.su/products/indaccel/elv.en.pdf>

A scheme for laser vacuum window

We suggest the following laser window design that is close to the foil design in the previous chapter (Fig. 5). Moving stock, driven by a motor, synchronously rotates two laser mirrors back and forth. This causes laser beam to scan across vacuum window, distributing heat load over a larger area. Vacuum window in this case should be made of rectangular shape.

Some advantages of this scheme are:

- Less heat per unit area on the window
- Flexibility: rotation can be switched on and off depending on the laser wavelength and power

Main disadvantage of this scheme is:

- Moving parts in vacuum (bellow lifetime)

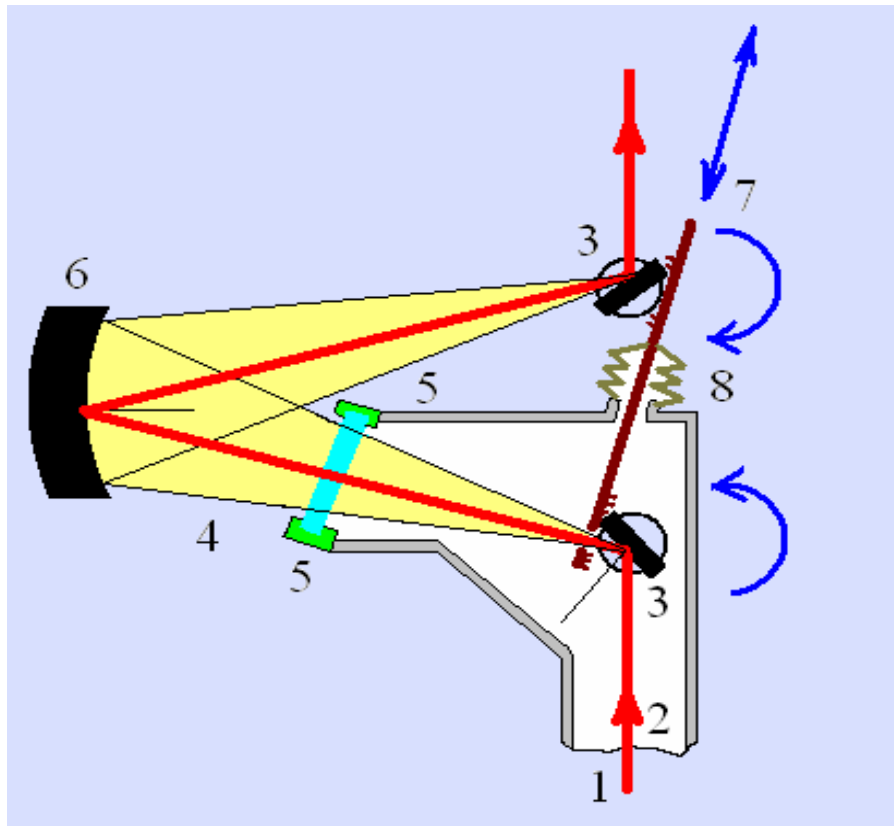


Fig: 5: 1 – incoming laser beam, 2 – vacuum tank, 3 – mirrors on rotating support, 4 – vacuum window, 5 – window holder, 6 – curved mirror, 7 – moving stock, 8 – bellow.

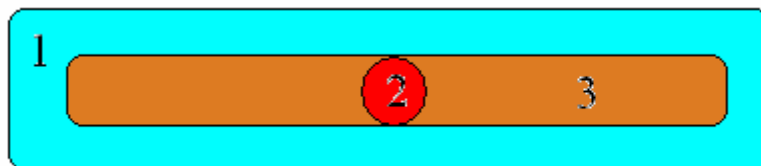


Fig. 6: Front view: 1 – window, 2 – beam profile, 3 – area occupied by the laser light when mirrors are rotated.

Thermal properties

The benefit of the suggested scheme is in distribution of the absorbed heat over a large area. As shown in Fig. 6, the area covered by the moving spot is much larger than the beam size. Thus, the power load per unit area will be decreased:

$$\frac{P_3}{P_2} \approx \frac{A_2}{A_3},$$

where P stands for the power per unit area, and A is the area.

Simpler solution is in defocusing of the radiation beam to a larger size⁴. Let us compare the “swiping” scheme with the “defocusing” one. We assume normal distribution of power as shown in Fig. 3. For a “defocusing mirror” scheme the power per unit surface is:

$$P(x, y) = \frac{P_0}{2\pi\sigma_x\sigma_y} \exp\left(-\frac{x^2}{2\sigma_x^2}\right) \exp\left(-\frac{y^2}{2\sigma_y^2}\right),$$

where σ_x , σ_y are horizontal and vertical beam sizes respectively.

For the “swiping” scheme the power distribution is given by the following expression:

$$P(x, y) = \frac{P_0}{2\pi\sigma_x\sigma_y 2L} \int_{-L}^L \exp\left(-\frac{(x-t)^2}{2\sigma_x^2}\right) dt \cdot \exp\left(-\frac{y^2}{2\sigma_y^2}\right),$$

where $2L$ is the swiping range.

In the following we assume that 100 kW beam is defocused along horizontal dimension only (rectangular window is used). For the “defocusing” scheme we take $\sigma_x=30$ mm, $\sigma_y=10$ mm (beam size is increased three times horizontally). For the “swiping” scheme we take a beam with $\sigma_x=\sigma_y=10$ mm and swiping range $L=76$ mm. The following figures show the power distributions (power is integrated along vertical axis).

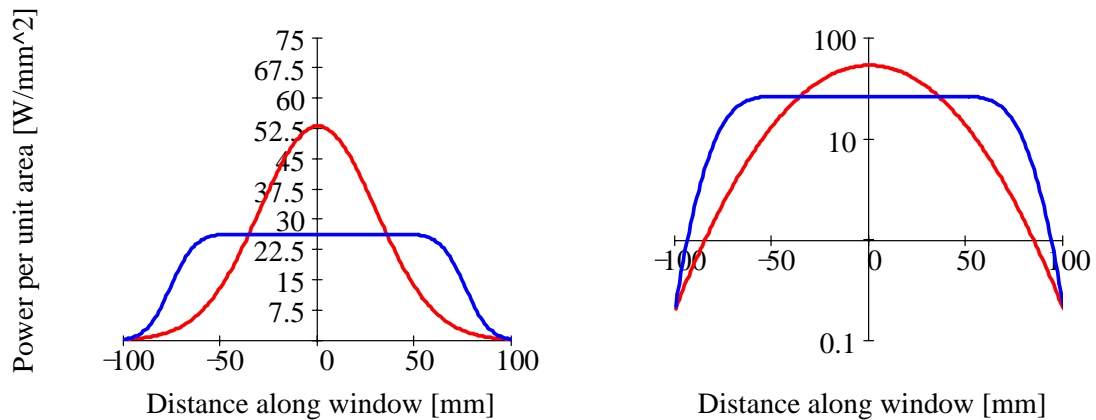


Fig. 7: Power distributions for the “defocusing” (red) and “swiping” (blue) schemes. Left plot is the same as the right one but in log scale.

⁴ N.A. Vinokurov, Private communication.

From this figure we may conclude that the power per unit area is twice as smaller for the “swiping” scheme than for the “defocusing” scheme. Note that we made the amounts of power to be the same at the edges of the window for both schemes (right plot).

Next we make a coarse estimate for the swiping speed of the system. We assume that the radiation power in the spot with the radius of 1 cm is 100 kW. The radiation passes through ZnSe vacuum window (bulk material absorption of 10^{-3} at 10.6 μm [⁵]) with the thickness of 1 cm and the horizontal dimension of 20 cm. For 1 second the temperature change of the material inside the spot is:

$$\Delta T = \frac{P \cdot A \cdot \Delta t}{\rho \cdot \pi \sigma^2 \cdot h \cdot c} = \frac{100 \text{ kW} \cdot 10^{-3} \cdot 1 \text{ s}}{5.27 \cdot 10^3 \text{ kg/m}^3 \cdot 3.14 \cdot 0.01^2 \cdot 0.01 \cdot 335 \text{ J/kg/K}} = 18 \text{ K}$$

The ZnSe material properties are taken from [⁶]. The temperature change of 18 degrees does not seem large (however, the steady-state temperature of the window material should be estimated). For the swiping speed we assume that in one second the radiation spot travels across the window on the distance equal to one spot size. Then the radiation spot will move across the whole window (20 cm) during ~20 seconds.

We note, however, that in this “order-of-magnitude” estimate no cooling was taken into account. The realistic analysis of the temperature dependence must include cooling and heat transfer, smooth distribution of power in the radiation spot, relaxation of the temperature between cycles, start-up regime, etc.

Optical properties

Since the central mirror is convex, it provides focusing of the beam horizontally that is desirable to compensate. The straightforward way of doing it is to make the other two mirrors defocusing. We write the transport matrix for a single mirror as:

$$M = \begin{vmatrix} 1 & 0 \\ -2/R & 1 \end{vmatrix},$$

where R is the radius of curvature and the mirror is assumed to be focusing. Then for the whole system we get:

$$M_s = \begin{vmatrix} 1 & 0 \\ -2/R_1 & 1 \end{vmatrix} \cdot \begin{vmatrix} 1 & L \\ 0 & 1 \end{vmatrix} \cdot \begin{vmatrix} 1 & 0 \\ -2/R_0 & 1 \end{vmatrix} \cdot \begin{vmatrix} 1 & L \\ 0 & 1 \end{vmatrix} \cdot \begin{vmatrix} 1 & 0 \\ -2/R_1 & 1 \end{vmatrix},$$

Using $R_1=2R_0=2L$, we obtain the focusing free optical system with the transport matrix equal to unity. Thus the 1st and the 2nd mirrors have to be made concaved.

For the vertical envelope this three-mirror system represents a drift space with no focusing. Thus vertical transport matrix will differ from horizontal one, which will induce some ellipticity into transverse radiation profile. This can be corrected by making the mirrors equally concaved vertically.

However, for some of the high-power lasers the output radiation Raleigh range may be significantly larger than the optical path length along the swiping system. In this case the ellipticity of the output radiation transverse profile is a minor effect.

⁵ http://optics.unicore.com/am4/docs/pdf/tdsulo_2_0.pdf

⁶ <http://www.crystran.co.uk/znsedata.htm>

Future work and conclusion

In the following we discuss some directions of future work on this scheme.

1. The scheme includes three mirrors. Reflection losses on the mirrors must be analyzed. We note, however, that in any case laser system may require several mirrors for the output beam alignment.
2. Brewster angle is changing while beam is being swiped across the window. This causes the radiation reflection to be greater to the edges of the window. It may not be a serious problem; in general, the change of angle should be small.
3. Effective glass thickness is changing from edge to edge; greater heat at the edges, unless curved window is used (will be similar in the “defocusing” case).
4. Speed of rotation should be estimated. The speed is determined by thermal conductivity of the window material.
5. Long mirror deformation under the heat should be calculated and corrected. It can be forced with a temperature stabilization circuit.
6. Coupled rotating mirrors scheme (“Rowland monochromator”).
7. “Defocusing mirror” option can be added by using vertical axis of the system (Fig. 5). All mirrors should be mounted on a platform that can be elevated or lowered. Curvature radii of all mirrors should smoothly vary along the vertical axis.
8. Rectangular window might be preferable as compared with a large round window. In the first case thickness of the window can be chosen to be less, having the same mechanical rigidity against atmospheric pressure. This will cause less absorption losses in the window material.

In conclusion we note that there is a number of FEL proposals, which consider the output laser power in a sub-MW to MW range⁷. The problem of radiation transport through the vacuum window may become a serious issue at this level of power. The scheme, discussed in this note, can provide with an effective solution of this problem.

Acknowledgements

I would like to thank N.A. Vinokurov, S. Benson and L.H. Yu for interesting and stimulating discussions on high-power FEL optics and windows.

⁷ <http://epaper.kek.jp/a01/PDF/TUBM04.pdf>
<http://uspas.fnal.gov/materials/Neil-Merminga.pdf>
<http://fel2004.elettra.trieste.it/pls/fel2004/Proceedings.html>
http://www.jlab.org/div_dept/admin/publications/papers/01/ACT01-21.pdf